

Controlling energy transfer time between two coupled magnetic vortex-state disks

H. Vigo-Cotrina¹ and A.P. Guimarães¹

Centro Brasileiro de Pesquisas Físicas, 22290-180, Rio de Janeiro, RJ, Brazil

(Dated: 11 May 2019)

The influence of the in-plane uniaxial anisotropy (IPUA) in the mutual energy transfer time (τ) between two identical coupled nanodisks was studied. Using an analytical dipolar model we obtained the interactions between the disks along x and y directions (the coupling integrals) as a function of the uniaxial anisotropy constant (K_σ) and the distance. We find that the IPUA increases the interaction between the disks allowing shorter energy transfer times. For our range of K_σ values we get a drop in the values of τ of up to about 70%. From the lagrangian of the system we obtained the equations of motion and the coupling frequencies of the dynamic system as a function of distance and K_σ . The coupling frequencies were also obtained from micromagnetic simulations. Our results of the simulations are in agreement with the analytical results.

I. INTRODUCTION

Depending on their geometries and sizes, magnetic nanostructures can present a vortex configuration as their ground states.^{1,2} This configuration is characterized by curling magnetization in the plane of the nanostructure, and a core where the magnetization points out of the plane. The curling direction defines the circulation $C = +1$ (counterclockwise (CCW)) and $C = -1$ (clockwise (CW)). The core has polarity $p_0 = +1$ when it points in the $+z$ direction and $p_0 = -1$ in the $-z$ direction. The magnetic vortices have several potential applications for devices, such as media for magnetic random access memories (MRAM), spin torque induced magnetization processes, microdisks for targeted cancer-cell destruction, etc.²⁻⁵

When vortices are excited from their equilibrium position and allowed to relax, they perform a motion called gyrotropic, with an eigenfrequency (gyrotropic frequency) in the sub-gigahertz range.^{1,2,6-8} This eigenfrequency depends on the ratio of the thickness to the radius of the disk ($\beta = L/R$).^{2,7} The control of gyrotropic frequency values has been reported in previous works using perpendicular magnetic fields and polarized spin current.⁹⁻¹¹ Nevertheless, problems such as the Joule heating and stray magnetic fields are undesirable for device applications¹², therefore a new mechanism for controlling the frequencies is needed. In this sense the influence of perpendicular uniaxial anisotropy (PUA) and in-plane uniaxial anisotropy (IPUA) in the magnetization process of magnetic vortices has gained interest in recent years.¹³⁻¹⁹ In multilayer systems a perpendicular uniaxial anisotropy (PUA) can be induced varying the substrate thickness¹⁸, while IPUA can be induced through inverse magnetostriction effect by voltage-induced strain via a PZT piezoelectric transducer^{14,20}. The IPUA allows real-time control of the eigenfrequency in an appreciable range¹³. The eigenfrequency can also be controlled using PUA, as has already been demonstrated by Fior *et al.*¹⁹, but the downside is that this control cannot be made in real-time, and the range of frequency variation is barely 3% before the vortex is destabilized.

When magnetic disks are close to one another, there arises a frequency splitting due to the magnetic interaction²¹. Expressions for the magnetic vortex excitation frequencies and coupling integrals in a pair of coupled circular disks of equal radii were obtained by Shibata *et al.*²¹ and Sukhostavets *et al.*²² These expressions were also obtained for the case of coupled circular disks of different radii by Sinnecker *et al.*²³

Coupling different disks with magnetic vortices allows the possibility of loss-less energy transfer between them²⁴, and the propagation of the information,²⁵ which is relevant for the flow of information in devices using magnetic vortices. The energy transfer time of a disk to the other is characterized by the parameter τ . This parameter is inversely proportional to the splitting frequency ($\Delta\omega/2\pi$).²⁴ In this sense, the control of the mutual energy transfer time τ is very important to characterize this transfer.

The goal of this work is to propose a novel method for controlling τ in a pair of identical nanodisks, using the influence of the IPUA. To date there is only one method of controlling the value of τ , using perpendicular magnetic fields²⁶. We used micromagnetic simulations and found a correlation between the IPUA values and τ . The coupling integrals I_x and I_y between disks and the splitting frequency are also affected by the presence of the IPUA. In order to gain physical meaning and obtain the new values of the coupling integral and splitting frequency, a simple analytic method considering dipolar interaction was used. Our analytical results are in accordance with the micromagnetic simulations.

The micromagnetic simulations were made using the open source software Mumax²⁷. The magnetoelastic energy was included in the micromagnetic simulation as a uniaxial anisotropy energy, as proposed in reference 13. We used cells of $2 \times 2 \times 7 \text{ nm}^3$. The magnetostrictive material used was Galfenol (FeGa), which is of great interest and exhibits high magnetostriction²⁰. The material parameters of Galfenol used here were^{13,28,29}: saturation magnetization $M_s = 1.360 \times 10^6 \text{ A/m}^2$, exchange stiffness $A = 14 \times 10^{-12} \text{ J/m}$. We used gyromagnetic ratio $\gamma = 2.21 \times 10^5 \text{ m/As}$, damping constant $\alpha = 0.01$

and IPUA ranging from 0 to 58500 J/m³. For larger values of the anisotropy, the magnetic vortex configuration is not stable. We used two identical disks, located along the x-axis, with diameters 256 nm, thickness L = 7 nm and separation distance D between the disks (Fig. 1). All our simulations were made considering uniaxial anisotropy in the direction of the x axis .

II. RESULTS AND DISCUSSION

A. Micromagnetic simulations

The gyrotropic frequency variation depending on the induced uniaxial anisotropy constant K_σ for an isolated disk has already been studied in detail by Roy¹³ for the same geometry that we used, however, we will make a brief description of this case.

The vortex core is initially at the equilibrium position, at the center of the disk. In order to induce gyrotropic movement, we first apply a static field of 20 mT in the +x direction for a few nanoseconds using a large damping $\alpha = 1$ for faster convergence, then this field is turned off and a typical damping $\alpha = 0.01$ was used, allowing the vortex core to perform the gyrotropic motion. The eigenfrequency ($f_0 = \omega_0/2\pi$) is obtained by a fast Fourier transform (FFT) from the time evolution of the magnetization. The frequency decrease with increasing anisotropy, as shown in Fig. 2.

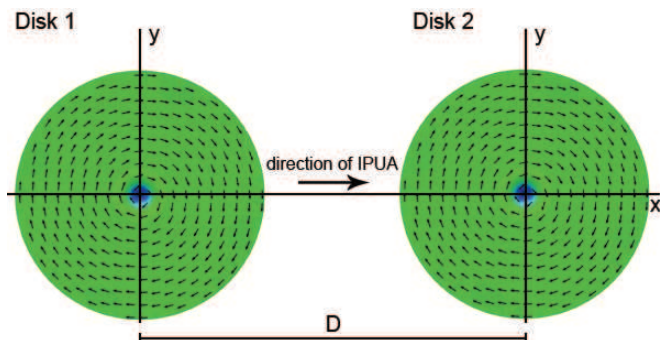


FIG. 1. Coupled disks with magnetic vortex configuration separated by a center-to-center distance D.

The gyrotropic frequencies can also be determined analytically using the linearized Thiele's equation³⁰. Considering a small damping, this equation can be written as:

$$\mathbf{G} \times \frac{d\mathbf{X}}{dt} - \frac{\partial W(\mathbf{X})}{\partial \mathbf{X}} = 0, \quad (1)$$

where \mathbf{G} is the gyrovector $\mathbf{G} = -Gp_0\hat{z}$, $G = 2\pi\mu_0M_sL/\gamma$ is the gyrotropic constant (it is assumed that the magnetization does not vary along the thickness of the disk,

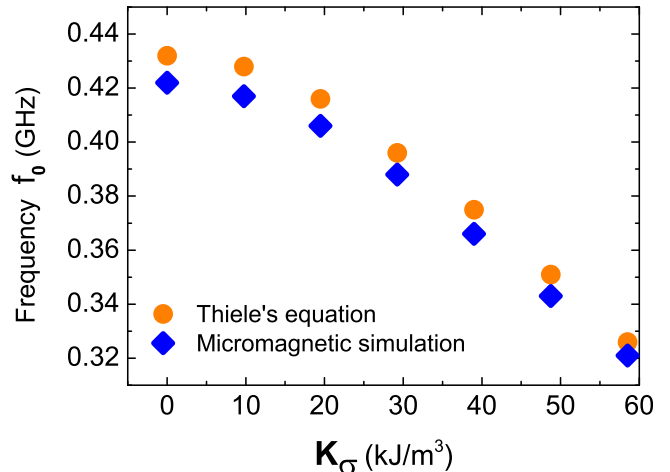


FIG. 2. Gyrotropic frequency variation with respect to K_σ for a isolated disk of diameter $2R = 256$ nm and thickness $L = 7$ nm. Blue diamonds and orange dots represent the values obtained from micromagnetic simulations, and Thiele's equation ($\kappa(2\pi G)^{-1}$), respectively.

an assumption valid for $\beta = L/R \ll 1$), γ is the gyromagnetic ratio and M_s is the saturation magnetization; $W(\mathbf{X}) = W(0) + \frac{1}{2}\kappa\mathbf{X}^2$ is the potential energy and $\kappa = 40\pi M_s^2 L^2/9R$ is the stiffness coefficient calculated within the side-charge-free model at $\beta \ll 1$, and R is the disk radius. The gyrotropic frequency is given by the expression $f_0 = \kappa(2\pi G)^{-1}$. The stiffness coefficient and the gyrotropic constant were obtained from micromagnetic simulations following the methodology of some previous works.^{13,26,31} Thus, the gyrotropic constant was obtained using the expression³¹:

$$G = \frac{L}{\gamma M_s^2} \int_S \mathbf{M} \cdot \left[\left(\frac{\partial \mathbf{M}}{\partial x} \right) \times \left(\frac{\partial \mathbf{M}}{\partial y} \right) \right] dS \quad (2)$$

and the stiffness coefficient was obtained from the slope of the linear fits of $W(\mathbf{X})$ versus \mathbf{X}^2 .^{9,13} The values of the gyrotropic constant and stiffness coefficient obtained from the analytical expressions are $G = 3.401 \times 10^{-13}$ kg/s and $\kappa = 9.86$ N/m for $K_\sigma = 0$ kJ/m³ while the values obtained from micromagnetic simulations are 3.375×10^{-13} kg/s and $\kappa = 9.16$ N/m. There is a good agreement between the results obtained from the analytical expressions and those obtained from micromagnetic simulation. With the presence of the IPUA the value of the gyrotropic constant remains unchanged, as shown in Fig. 3, which means that the IPUA does not alter the profile of the vortex core¹³, whereas the stiffness coefficient shows a falling value with increasing anisotropy constant K_σ . This fall is due to the competition between exchange and demagnetizing energy versus magnetoelastic energy¹³. Decreasing kappa values are reflected in the values of the eigenfrequencies, as shown in Fig. 2. Our results obtained for isolated disks are consistent with those obtained by Roy¹³.

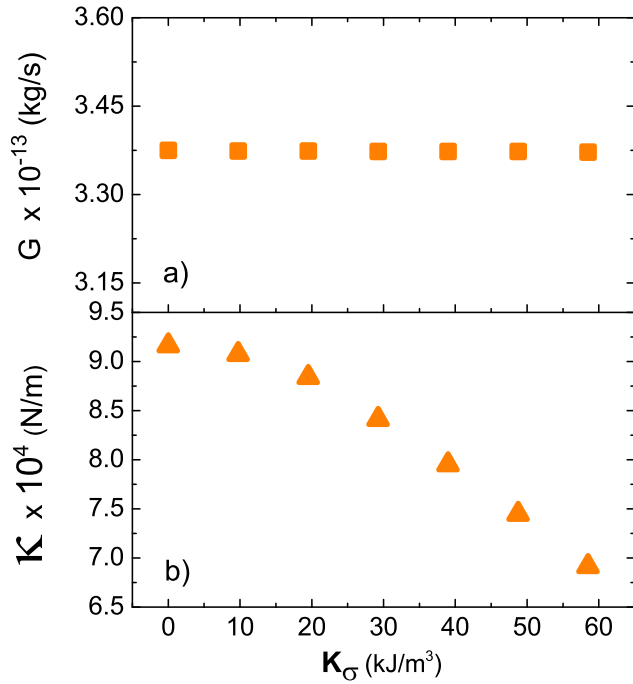


FIG. 3. a) Gyrotropic constant G and b) stiffness coefficient κ obtained from micromagnetic simulations.

In order to study the dependence of τ with the IPUA, we considered a system of two coupled disks, located along the x-axis, separated by a center to center distance D , as shown in Fig. 1. Initially, both vortex cores are in the equilibrium position at the center of their respective disks. In order to induce gyrotropic movement we have applied a static field in the $+x$ direction for a few nanoseconds only on disk 1, then this field was turned off, allowing the vortex core to perform the gyrotropic motion with decreasing amplitude, while the vortex core of disk 2 begins to perform the gyrotropic movement with increasing amplitude, due to transfer of energy from disk 1.

The splitting frequency is affected by the presence of the IPUA, increasing with the increase of K_σ from 19.35 MHz ($K_\sigma = 0 \text{ kJ/m}^3$) to 55.9 MHz ($K_\sigma = 58.5 \text{ kJ/m}^3$) for the case $p = p_1 p_2 = +1$. For $p = -1$ the splitting frequency increases from 48.25 MHz ($K_\sigma = 0 \text{ kJ/m}^3$) to 66.8 MHz ($K_\sigma = 58.5 \text{ kJ/m}^3$). This dependence is shown in Fig. 4. As expected, the splitting frequency is larger for the case $p = -1$ than for $p = +1$ because the dipolar interaction is stronger in the former case²⁵.

Since the splitting frequency ($\Delta\omega/2\pi$) is inversely related to the energy transfer time (τ)²⁴, it is expected that τ also depends on K_σ . This dependence is shown in Fig. 4 for $p = +1$ and $p = -1$. These values were extracted from micromagnetic simulations considering the τ definition: τ is defined as the time required by the energy of disk 1 to reach its minimum value for the first time²⁴. Additionally, we have calculated τ using the expression

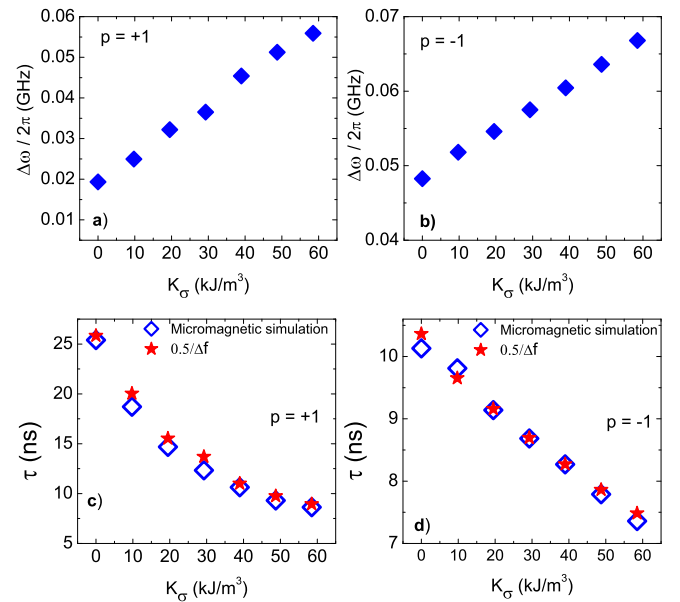


FIG. 4. Splitting frequency and τ variation with respect to K_σ for a) $p = +1$, and b) $p = -1$ with reduced distance $d = D/R = 2.27$, both obtained from micromagnetic simulations.

$\tau = 0.5/\Delta f$ ²⁴, where $\Delta f = \Delta\omega/2\pi$. These results are also shown in Fig. 4. Another way to find the τ values is to observe the time required for envelopes of \mathbf{X}_1 or $\mathbf{M}_1(t)$ reach their minimum values for the first time. In all cases, the results are almost the same. For a reduced distance $d = D/R = 2.27$, we found a drop in the value of τ of almost 69%, from $\tau = 25.4 \text{ ns}$ ($K_\sigma = 0$) to $\tau = 8.6 \text{ ns}$ ($K_\sigma = 58.5 \text{ kJ/m}^3$) for $p = +1$ and a drop of 27% from $\tau = 10.13 \text{ ns}$ ($K_\sigma = 0$), to $\tau = 7.36 \text{ ns}$ ($K_\sigma = 58.5 \text{ kJ/m}^3$) for $p = -1$. For larger d , the decrease in the value of τ with respect to the increase of K_σ remains significant (approximately 60%) for $p = +1$, while for the case $p = -1$ the drops are reduced to 20%. Despite getting lower values of τ with high values of K_σ , it is important to note that energy transfer times remain shorter when $p = -1$. This is because the coupling between the two disks is stronger in comparison with $p = +1$ ²⁶. Up to this point we have shown that it is possible to control the energy transfer time using the influence of the IPUA, thus becoming a new and effective method for controlling τ . Next, we will explain the reason why τ decreases with increasing K_σ .

B. Analytical dipolar model

Although the magnetic interaction between magnetic vortices depends on several multipole terms³², we used a simple dipolar model to understand the effect of IPUA on the coupling integrals. This model has been used in other work for the study of the magnetic interaction among three coupled disks system³³. The magnetic dipolar en-

ergy (E_{dip}) is given by:

$$E_{dip} = \frac{\mu_0}{4\pi D_{ij}^3} [\boldsymbol{\mu}_i \cdot \boldsymbol{\mu}_j - 3(\hat{\mathbf{D}}_{ij} \cdot \boldsymbol{\mu}_i)(\hat{\mathbf{D}}_{ij} \cdot \boldsymbol{\mu}_j)], \quad (3)$$

where $\hat{\mathbf{D}}_{ij}$ is a unit vector along the axis connecting the centers of the disks i and j .

For small displacements, the magnetic dipolar moment for a magnetic vortex is defined by:³³

$$\boldsymbol{\mu}_{i,j} = -\lambda C_{i,j} M_s LR (\hat{\mathbf{z}} \times \mathbf{X}_{i,j}), \quad (4)$$

with:

$$\lambda_{i,j} = \frac{\pi R \|M_{i,j}\|}{M_s \|X_{i,j}\|} \quad (5)$$

where λ (in our case, $\lambda_i = \lambda_j$ because the two disks have the same dimensions) is a parameter that depends on the position and the magnetization of the vortex core which can be extracted from micromagnetic simulations, $C_{i,j}$ is the circulation of the disks i and j , $\mathbf{X}_{i,j} = (x_{i,j}, y_{i,j})$ is the vector position of the core vortex of the disks. After some algebra and considering $i, j = 1, 2$ we obtain the following expression for the magnetic dipolar energy:

$$E_{dip} = C_1 C_2 (\eta^* x_1 x_2 - 2\eta^* y_1 y_2), \quad (6)$$

where $\eta^* = \mu_0 \lambda^2 M_s^2 L^2 R^2 / 4\pi D_{12}^3$, $D_{12} = D$ is the center-to-center distance between 2 disks. Eq. (6) is similar to the analytical expression obtained for the magnetic interaction energy (W_{int}) given by:^{21,22}

$$W_{int} = C_1 C_2 (\eta_x x_1 x_2 + \eta_y y_1 y_2), \quad (7)$$

Comparing Eq. (6) with Eq. (7) we obtain:

$$\eta_x = \eta^* \quad \eta_y = -2\eta^* \quad (8)$$

Therefore, the new coupling integrals are given by:

$$I_{x,y} = \frac{8\pi}{\mu_0 R M_s^2} \eta_{x,y} \quad (9)$$

The expressions of the coupling integral obtained in previous works are limited to the case when the magnetic vortex configuration is not disturbed by some external agent (e.g.: perpendicular magnetic field, perpendicular uniaxial anisotropy, IPUA). In contrast, our expressions for the coupling integrals (Eq. 9) can be used when the magnetic vortex configuration is disturbed, as they depend on the λ parameter, that is unique for each level of disturbance. In order to obtain the λ parameter, we follow the methodology used by Asmat *et al.*³³. In an isolated disk, the vortex core is displaced from the center of

the disk for the \mathbf{X} position by application of an in-plane magnetic field and considering a large damping ($\alpha = 1$) for faster convergence; in this position we measured the magnetization \mathbf{M} . Knowing these two quantities, we can now make use of Eq. 5. We repeat the same procedure for each value of K_σ . In the linear regime, the magnetization \mathbf{M} and \mathbf{X} are proportional²², therefore the λ parameter is independent of time and it has an unique value for each K_σ .

Accordingly, we find the values of the coupling integrals; these results are shown in Fig. 5. For $d = 2.27$ and $K_\sigma = 0$ kJ/m³ the ratio $\|I_y\|/I_x$ is approximately 0.38 using expressions obtained by Shibata *et al.*²¹, whereas if we use Eq. 9 the ratio is 0.5. This difference is expected because our model only considers the dipolar term in the interaction energy (Eq. 3), however for larger d the ratio $\|I_y\|/I_x$ begins to approach 0.5.

Considering our expressions for the coupling integrals (Eq. 9), we will determine the expression for the eigenfrequencies (or coupling frequencies) of the two disks coupled system.

The lagrangian expression for a pair of coupled disks based on the constant of the Thiele's equation is defined by:^{33,34}

$$\mathcal{L} = -\frac{1}{2} \sum_i^j \{G p_i (x_i \dot{y}_i - y_i \dot{x}_i) - \kappa |\mathbf{X}_i|^2\} - \sum_{i < j} E_{dip}^{ij}, \quad (10)$$

From the first variation of the lagrangian (Eq. 10) we obtained the equations of motion:

$$\begin{bmatrix} \dot{x}_1 \\ \dot{x}_2 \\ \dot{y}_1 \\ \dot{y}_2 \end{bmatrix} = \frac{1}{G} \begin{bmatrix} 0 & 0 & p_1 \kappa & -2p_1 \eta^* \\ 0 & 0 & -2p_2 \eta^* & p_2 \kappa \\ -p_1 \kappa & -p_1 \eta^* & 0 & 0 \\ -p_2 \eta^* & -p_2 \kappa & 0 & 0 \end{bmatrix} \begin{bmatrix} x_1 \\ x_2 \\ y_1 \\ y_2 \end{bmatrix} \quad (11)$$

The coupling frequencies (or eigenfrequencies) are obtained from Eq. 11:

$$\omega_{1,2} = \sqrt{\omega_0^2 - 2p \left(\frac{\eta^*}{G}\right)^2 \pm \frac{\eta^*}{G} \omega_0 \sqrt{5 - 4p}} \quad (12)$$

and the splitting frequency:

$$|\omega_2 - \omega_1| = \sqrt{2} \omega_0 \sqrt{1 - 2pu^2 - \sqrt{4u^4 - 5u^2 + 1}} \quad (13)$$

where ω_0 is an eigenfrequency of an isolated disk and $u = \eta^*/G\omega_0$.

The coupling frequencies do not depend on the sign of the circulations C_1 and C_2 , they depend only on the combination of polarities ($p = +1$ or $p = -1$).

The dependence of the coupling integrals on K_σ and reduced separation distance d is shown in Fig. 5. The values of the coupling integrals increase with increasing K_σ , meaning that the presence of IPUA favors the appearance of magnetic charges, making the coupling between both disks stronger. This result is very important because as the coupling integrals increase, the splitting frequency also increases (see Eq. 13), therefore τ must decrease (previous Section). This explains why τ decreases with increasing K_σ , as already discussed in the previous section. The effects caused by the IPUA strongly contrast to those produced by perpendicular magnetic fields. While it is true that in the case of an isolated disk, both the IPUA and the application of a perpendicular magnetic field antiparallel to the polarity of the vortex produce the same effect of decreasing frequency, it is not the same in the case of coupled disks. τ increases with the increase of the applied perpendicular magnetic field, while it decreases with increasing K_σ . The reason for this is that the perpendicular magnetic field deforms the core profile of the vortex, making the coupling integrals weak²⁶ while the presence of IPUA does not alter the core profile of the vortex¹³. As expected, the values of the coupling integrals decrease with the increase of the center-to-center distance of the disks.

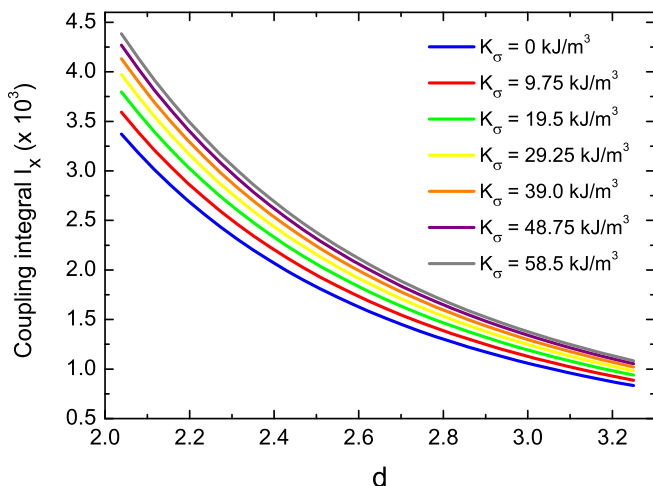


FIG. 5. Coupling integral I_x as a function of the reduced distance $d = D/R$ for disks with $L = 7$ nm and diameter 256 nm. These results were obtained from Eq. (9).

In order to test Eq. 12, we compared the coupling frequencies of the two-coupled disk system obtained from micromagnetic simulations with the results obtained using Eq. 12. These results are shown in Fig. (6) for $K_\sigma = 58.5$ kJ/m³ and for the combination of polarities $p = +1$ and $p = -1$. As our model considers purely dipolar interaction, which is far-reaching, it is expected that this is well-behaved when the separation distance between the disks is larger, as shown in Fig. 6. Although it is necessary to make some adjustments to our model to improve efficiency for small separation distances where high-order

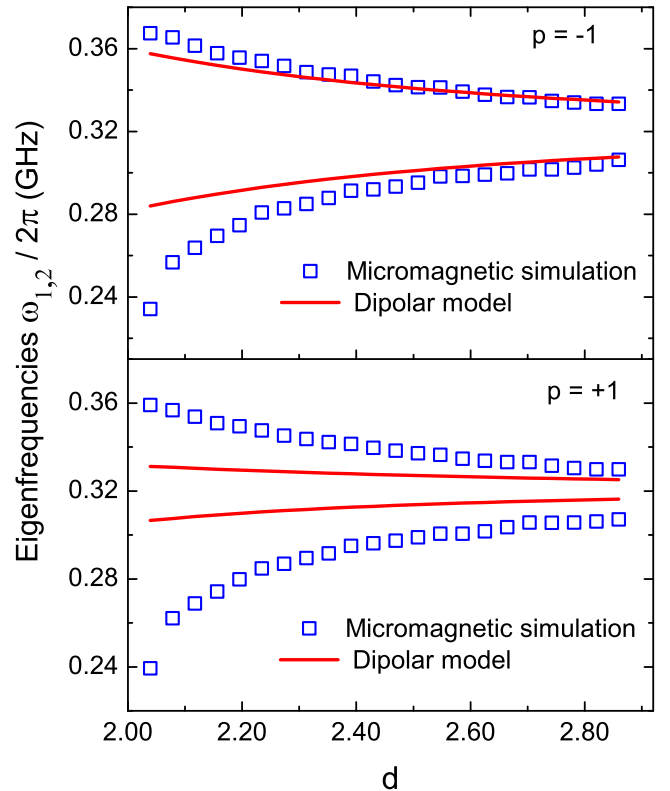


FIG. 6. Variation of coupling frequencies $\omega_{1,2}/2\pi$ with the reduced distance $d = D/R$ between two disks with combined polarities $p = +1$ and $p = -1$ for $K_\sigma = 58.5$ kJ/m³. The blue squares represent the values obtained from micromagnetic simulations and the red solid line represents the values obtained from Eq. (12).

magnetic interactions, such as dipole-octupole, octupole-octupole, dipole-triacontadipole are appreciable³², it is sufficient to explain the influence of the IPUA in the interaction between two disks.

III. CONCLUSION

In this work we have studied the influence of the IPUA on an isolated disk and on a system of coupled identical disks, both with a magnetic vortex configuration. In the isolated disk system, we have obtained the gyrotropic frequency, gyrotropic constant and stiffness constant from micromagnetic simulations. In the two coupled disks system, using micromagnetic simulations, we demonstrated that it is possible to control the mutual energy transfer time using the IPUA, introducing a new method for controlling τ . Using a simple analytical dipolar model, we have obtained the coupling integrals (interactions in the x and y directions) depending on the reduced separation distance d and K_σ . Also, we were able to explain why τ decreases with increasing K_σ , and clarify the difference in using perpendicular magnetic fields and IPUA. We have also analytically found the coupling frequencies

and compared this with the coupling frequencies obtained from micromagnetic simulations. Our analytical results are consistent with those obtained by micromagnetic simulation.

ACKNOWLEDGMENTS

The authors would like to thank the support of the Brazilian agencies CNPq and FAPERJ.

- ¹K. Y. Guslienko, *J. Nanoscience Nanotechnol.* **8**, 2745 (2008).
- ²A. P. Guimarães, *Principles of Nanomagnetism* (Springer, Berlin, 2009).
- ³N. Locatelli, V. Cros, and J. Grollier, *Nat. Mater.* **13**, 1476 (2014).
- ⁴S. Bohlens, B. Krüger, A. Drews, M. Bolte, G. Meier, and D. Pfannkuche, *Appl. Phys. Lett.* **93**, 142508 (2008).
- ⁵A. D. Belanovsky, N. Locatelli, P. N. Skirdkov, F. Abreu Araujo, K. A. Zvezdin, J. Grollier, V. Cros, and A. K. Zvezdin, *Appl. Phys. Lett.* **103**, 122405 (2013).
- ⁶V. Novosad, F. Y. Fradin, P. E. Roy, K. S. Buchanan, K. Y. Guslienko, and S. D. Bader, *Phys. Rev. B* **72**, 024455 (2005).
- ⁷K. Y. Guslienko, X. F. Han, D. J. Keavney, R. Divan, and S. D. Bader, *Phys. Rev. Lett.* **96**, 067205 (2006).
- ⁸V. Novosad, M. Grimsditch, K. Y. Guslienko, P. Vavassori, Y. Otani, and S. D. Bader, *Phys. Rev. B* **66**, 052407 (2002).
- ⁹M.-W. Yoo, K.-S. Lee, D.-S. Han, and S.-K. Kim, *J. Appl. Phys.* **109**, 063903 (2011).
- ¹⁰Y.-S. Choi, S.-K. Kim, K.-S. Lee, and Y.-S. Yu, *Appl. Phys. Lett.* **93**, 182508 (2008).
- ¹¹G. de Loubens, A. Riegler, B. Pigeau, F. Lochner, F. Boust, K. Y. Guslienko, H. Hurdequint, L. W. Molenkamp, G. Schmidt, A. N. Slavin, V. S. Tiberkevich, N. Vukadinovic, and O. Klein, *Phys. Rev. Lett.* **102**, 177602 (2009).
- ¹²S. A. Cavill, D. E. Parkes, J. Miguel, S. S. Dhesi, K. W. Edmonds, R. P. Champion, and A. W. Rushforth, *Appl. Phys. Lett.* **102** (2013), <http://dx.doi.org/10.1063/1.4789396>.
- ¹³P. E. Roy, *Appl. Phys. Lett.* **102**, 162411 (2013).
- ¹⁴T. A. Ostler, R. Cuadrado, R. W. Chantrell, A. W. Rushforth, and S. A. Cavill, *Phys. Rev. Lett.* **115**, 067202 (2015).
- ¹⁵S. Parreiras and M. Martins, *Phys. Proc.* **75**, 1142 (2015).
- ¹⁶E. R. P. Novais, P. Landeros, A. G. S. Barbosa, M. D. Martins, F. Garcia, and A. P. Guimarães, *J. Appl. Phys.* **110**, 053917 (2011).
- ¹⁷E. R. P. Novais, S. Allende, D. Altbir, P. Landeros, F. Garcia, and A. P. Guimarães, *J. Appl. Phys.* **114**, 153905 (2013).
- ¹⁸F. Garcia, H. Westfahl, J. Schoenmaker, E. J. Carvalho, A. D. Santos, M. Pojar, A. C. Seabra, R. Belkhou, A. Bendounan, E. R. P. Novais, and A. P. Guimarães, *Appl. Phys. Lett.* **97**, 022501 (2010).
- ¹⁹G. B. M. Fior, E. R. P. Novais, J. P. Sinnecker, A. P. Guimarães, and F. Garcia, *J. Appl. Phys.* **119**, 093906 (2016).
- ²⁰D. E. Parkes, L. R. Shelford, P. Wadley, V. Hol, M. Wang, A. T. Hindmarch, G. van der Laan, R. P. Champion, K. W. Edmonds, S. A. Cavill, and A. W. Rushforth, *Sci. Rep.* **3**, 2220 (2013).
- ²¹J. Shibata, K. Shigeto, and Y. Otani, *Phys. Rev. B* **67**, 224404 (2003).
- ²²O. V. Sukhostavets, J. M. Gonzalez, and K. Y. Guslienko, *Appl. Phys. Express* **4**, 065003 (2011).
- ²³J. P. Sinnecker, H. Vigo-Cotrina, F. Garcia, E. R. P. Novais, and A. P. Guimarães, *J. Appl. Phys.* **115**, 203902 (2014).
- ²⁴H. Jung, K.-S. Lee, D.-E. Jeong, Y.-S. Choi, Y.-S. Yu, D.-S. Han, A. Vogel, L. Bocklage, G. Meier, M.-Y. Im, P. Fischer, and S.-K. Kim, *Sci. Rep.* **1**, 59 (2011).
- ²⁵J.-H. Kim, K.-S. Lee, H. Jung, D.-S. Han, and S.-K. Kim, *Appl. Phys. Lett.* **101**, 092403 (2012).
- ²⁶D.-S. Han, Y.-J. Cho, H.-B. Jeong, and S.-K. Kim, *J. Appl. Phys.* **117**, 083910 (2015).
- ²⁷A. Vansteenkiste, J. Leliaert, M. Dvornik, M. Helsen, F. Garcia-Sanchez, and B. Van Waeyenberge, *AIP Advances* **4**, 107133 (2014).
- ²⁸T. Brintlinger, S.-H. Lim, K. H. Baloch, P. Alexander, Y. Qi, J. Barry, J. Melngailis, L. Salamanca-Riba, I. Takeuchi, and J. Cumings, *Nano Letters* **10**, 1219 (2010).
- ²⁹T. A. Summers, E. M. and Lograsso and M. Wun-Fogle, *J. Mat. Sci.* **42**, 9582 (2007).
- ³⁰A. A. Thiele, *Phys. Rev. Lett.* **30**, 230 (1973).
- ³¹Y.-S. Yu, D.-S. Han, M.-W. Yoo, K.-S. Lee, Y.-S. Choi, H. Jung, J. Lee, M.-Y. Im, P. Fischer, and S.-K. Kim, *Sci. Rep.* **3**, 1301 (2013).
- ³²O. V. Sukhostavets, J. González, and K. Y. Guslienko, *Phys. Rev. B* **87**, 094402 (2013).
- ³³M. Asmat-Uceda, X. Cheng, X. Wang, D. J. Clarke, O. Tchernyshyov, and K. S. Buchanan, *J. Appl. Phys.* **117**, 123916 (2015).
- ³⁴J. Shibata, Y. Nakatani, G. Tatara, H. Kohno, and Y. Otani, *Phys. Rev. B* **73**, 020403 (2006).